

Three Types of Ion Channels in the Cell Membrane of Mouse Fibroblasts

M. KOSELSKI¹, A. OLSZEWSKA², A. HORDYJEWSKA³, T. MALECKA-MASSALSKA², K. TREBACZ¹

¹Department of Biophysics, Institute of Biology and Biochemistry, Maria Curie-Skłodowska University, Lublin, Poland, ²Department of Human Physiology, Medical University of Lublin, Lublin, Poland, ³Department of Medical Chemistry, Medical University of Lublin, Lublin, Poland

Received April 1, 2016

Accepted July 15, 2016

On-line October 26, 2016

Summary

Patch clamp recordings carried out in the inside-out configuration revealed activity of three kinds of channels: nonselective cation channels, small-conductance K⁺ channels, and large-conductance anion channels. The nonselective cation channels did not distinguish between Na⁺ and K⁺. The unitary conductance of these channels reached 28 pS in a symmetrical concentration of 200 mM NaCl. A lower value of this parameter was recorded for the small-conductance K⁺ channels and in a 50-fold gradient of K⁺ (200 mM/4 mM) it reached 8 pS. The high selectivity of these channels to potassium was confirmed by the reversal potential (-97 mV), whose value was close to the equilibrium potential for potassium (-100 mV). One of the features of the large-conductance anion channels was high conductance amounting to 493 pS in a symmetrical concentration of 200 mM NaCl. The channels exhibited three subconductance levels. Moreover, an increase in the open probability of the channels at voltages close to zero was observed. The anion selectivity of the channels was low, because the channels were permeable to both Cl⁻ and gluconate – a large anion. Research on the calcium dependence revealed that internal calcium activates nonselective cation channels and small-conductance K⁺ channels, but not large-conductance anion channels.

Key words

Patch-clamp • Mouse fibroblast • Cell membrane • Cation channels • K⁺ channels • Anion channels

Corresponding author

M. Koselski, Department of Biophysics, Institute of Biology and Biochemistry, Maria Curie-Skłodowska University, Akademicka 19, 20-033 Lublin, Poland. E-mail: mateusz.koselski@poczta.umcs.lublin.pl

Introduction

Fibroblasts are the most common type of cells found in connective tissue. They are defined as cells that synthesize and secrete collagen proteins and they are also believed to be an essential source of many other extracellular matrix components (Theerakittayakorn and Bunprasert 2011). Animal or human fibroblasts grow well in cultures and are readily available for experiments; therefore, they have been widely used for investigation of many physiological and biochemical responses. Learning more about their general physiology and ion channel activity in particular is very important (Estacion 1991).

Different types of cation- and anion-selective channels were characterized in mouse fibroblasts using patch-clamp techniques. Voltage-dependent calcium currents were detected in mouse Swiss 3T3 fibroblasts (Peres *et al.* 1988a, Peres *et al.* 1988b). These rapidly activating and fully inactivating inward currents were evoked by depolarization from negative voltages and were similar to low-voltage T-type calcium channels activated by small depolarization of the cell membrane potential (Perez-Reyes 2003). Weak permeability of recorded channels to other than calcium divalent cations

was confirmed by reduction of the currents by Cd^{2+} (Peres *et al.* 1988a), and slight reduction of the currents recorded after replacement of external Ca^{2+} with Ba^{2+} (Peres *et al.* 1988b). On the other hand, after elimination of all divalent cations from the external solution, permeability to monovalent cations was observed. A lack of sensitivity to calcium channel blockers like nitrendipine and verapamil was also characteristic for the channels. In the study of Peres and coworkers, an absence of calcium-activated K^+ channels was reported (Peres *et al.* 1988a), but such channels were recorded in the mouse fibroblastic line LMTK-, a thymine-kinase-deficient strain of L cells (Hosoi and Slaymann 1985). In turn, cell-attached and inside-out patch recording carried out by Frace and Gargus indicated that the predominant channel of LMTK- was a nonselective calcium- and voltage independent cation channel, permeable equally to Na^+ , K^+ , and Cs^+ and non-permeable to anions or divalent cations (Frace and Gargus 1989). Apart from mouse LMTK-cells, Ca^{2+} dependent K^+ currents were recorded also in NIH3T3 mouse fibroblasts (Repp *et al.* 1998). The channels were activated by lysophosphatidic acid and showed voltage-independence and sensitivity to the K^+ channels blockers (charybdotoxin, margatoxin, and iberiotoxin). The whole cell patch-clamp recordings carried out in mouse LMTK-fibroblasts indicated existence of volume-sensitive Cl^- currents whose activation is delayed by high intracellular chloride (Doroshenko 1999). Moreover, Cl^- conductance of these channels is affected by protein tyrosine phosphatase inhibitors (Thoroed *et al.* 1999). Mouse skin fibroblasts 3T3-L1 were also used for patch-clamp investigations by Goodwin and coworkers. However, as reported, there were difficulties in obtaining results, since poor seals in both cell-attached and excised inside-out configurations and a low success rate in finding channels (<10 %) were observed. The channels, rarely recorded in the cell-attached configuration, were not voltage-dependent and probably K^+ impermeable (Goodwin *et al.* 1998).

Ion channels play an important physiological role. Many functions and possible roles of some channels are discussed. A big number of ion channelopathies, especially potassium, calcium, and sodium channel diseases, affect the neuromuscular system and cause diseases such as epilepsy, myotonia, or cardiac arrhythmias (Fiske *et al.* 2006). Defects in ion channels may cause either a gain or a loss of channel function. Changes in the ion channel composition have been observed in fibroblasts from patients with Alzheimer's disease (AD). Etcheberrigaray

and coworkers indicated an absence of a 113-pS tetraethylammonium (TEA)-sensitive K^+ channel in AD fibroblasts, while they were present in control cells (Etcheberrigaray *et al.* 1993).

This paper describes ion channels found in the mouse L929 fibroblastic cell line, which is widely used in many experimental aspects. Patch-clamp recordings carried out in the inside-out configuration allowed characterization of three different types of channels, which are important for transport of monovalent cations and anions through the cell membrane.

Materials and Methods

Cell culture and culture media

The experiment was conducted on a reference cell line L929 (cell line origin – mouse C3H/An connective tissue). The L929 cell line was obtained from ATCC (specification – NCTC clone 929 [L cell, L-929, derivative of Strain L] (ATCC® CCL-1™), http://www.lgcstandards-atcc.org/products/all/CCL-1.aspx?geo_country=pl). Cell cultures were grown at 37 °C in a humidified atmosphere comprising 5 % CO_2 in the air. L929 cultures were maintained at density of $2\text{-}4 \times 10^4$ cell/ml in exponential growth serum free conditions containing Modified Eagle Medium (MEM, Pan-Biotech, P04-08500; <http://www.pan-biotech.de/en/media-en/cell-culture-media/mem-overview/mem-with-earle-s-salts>) supplemented with 5 % fetal bovine serum (Pan-Biotech, P30-1985, <http://www.pan-biotech.de/en/sera/treated-sera>), 100 U/ml of penicillin, 100 µg/ml of streptomycin, 0.25 µg/ml of amphotericin B (Pan-Biotech, P06-07300; <http://www.pan-biotech.de/en/reagents/antibiotics-and-antifungal-drugs>), and routinely passaged every second day using 0.25 % trypsin (Pan-Biotech, P10-027500; <http://www.pan-biotech.de/en/reagents/enzymes-for-cell-dissociation/trypsin-and-others>). Cell viability was assessed by the ability to exclude trypan blue dye (Sigma-Aldrich, Germany, T6146). Cells for patch-clamp experiments were transferred to plastic 60-mm tissue culture dishes and grown in the same conditions for up 2 days.

Solutions used in the patch-clamp recordings

Patch-clamp recordings were made in the inside-out configuration in solutions initially containing symmetrical (in the pipette and in the bath) concentrations of 200 mM NaCl, 4 mM KCl, 2 mM CaCl_2 , 2 mM MgCl_2 , pH 7.3 buffered with 10 mM

HEPES/NaOH (abbreviation of these solutions used in figure legends and text – $200 \text{ Na}^+_{\text{pipette}}/200 \text{ Na}^+_{\text{bath}}$). The selectivity of the channels was examined in a NaCl gradient after tenfold reduction of NaCl in the bath by application of 20 mM NaCl, 4 mM KCl, 2 mM CaCl_2 , 2 mM MgCl_2 , pH 7.3 buffered with 10 mM HEPES/NaOH (abbreviation – $200 \text{ Na}^+_{\text{pipette}}/20 \text{ Na}^+_{\text{bath}}$). Permeability of cation-permeable channels to potassium was studied by replacement of NaCl in the bath with KCl – of 200 mM KCl, 4 mM NaCl, 2 mM CaCl_2 , 2 mM MgCl_2 , pH 7.3 buffered with 10 mM HEPES/KOH (abbreviation – $200 \text{ Na}^+_{\text{pipette}}/200 \text{ K}^+_{\text{bath}}$). Permeability of anion-permeable channels to gluconate was studied in 20 mM NaCl, 4 mM KCl, 2 mM CaCl_2 , 2 mM MgCl_2 , pH 7.3 buffered with 10 mM HEPES/NaOH in the bath and 200 mM Na-gluconate, 4 mM KCl, 2 mM CaCl_2 , 2 mM MgCl_2 , pH 7.3 buffered with 10 mM HEPES/NaOH in the pipette (abbreviation – $200 \text{ Glu}^-_{\text{pipette}}/32 \text{ Cl}^-_{\text{bath}}$). Calcium dependence of the channels was tested during inside-out recordings by application of the solution containing 2 mM Ca^{2+} (200 mM KCl, 4 mM KCl, 2 mM CaCl_2 , 2 mM MgCl_2 , pH 7.3 buffered with 10 mM HEPES/KOH) by a micropipette placed close to the cytoplasmic side of the cell membrane. Calcium was injected using a CellTram vario pump (Eppendorf, Hamburg). Before calcium application, the recordings were carried out in 200 mM NaCl, 4 mM KCl, 2 mM CaCl_2 , 2 mM MgCl_2 , pH 7.3 buffered with 10 mM HEPES/NaOH in the pipette and 200 mM KCl, 4 mM NaCl, 2 mM EGTA, 2 mM MgCl_2 , pH 7.3 buffered with 10 mM HEPES/KOH in the bath (abbreviation – $200 \text{ Na}^+, 2 \text{ Ca}^{2+}_{\text{pipette}}/200 \text{ K}^+, 2 \text{ EGTA}_{\text{bath}}$). The osmolarity of solutions with a reduced ionic concentration was compensated by adding sorbitol. Adjusting of the osmolarity was measured with a cryoscopic osmometer (Osmomat 030, Gonotec).

Patch-clamp measurements

The patch pipettes and micropipettes used for injection of Ca^{2+} were prepared from borosilicate glass capillary tubes with an outer diameter of 1.5 mm (Kwik-Fil, TW150-4, World Precision Instruments), pulled by a universal puller (DMZ). The patch pipette tip had an inside diameter of approx. 2 μm . An Ag-AgCl reference electrode filled with 100 mM KCl was connected with the bath solution *via* a ceramic porous bridge. The recordings were made by a patch-clamp amplifier EPC-10 (Heka Elektronik) coupled with the Patchmaster software (Heka Elektronik). The signals

were recorded with a frequency of 10 kHz and filtered at 2 kHz. The recordings, which lasted 10 s or more (Fig. 5), were drawn by taking into account every tenth measuring point. Elaboration of the current/voltage characteristics (I/V) and column diagrams showing dependence of the open probability on the voltage applied was made in SigmaPlot 9.0 (Systat Software Inc.). The slope of the I/V curve allowed calculation of the unitary conductance of the channels. Open probability of the channels was calculated in Fitmaster (Heka Elektronik).

Statistical analysis

Data presented in the I/V curves and P_o/V column charts are given as arithmetic mean \pm standard error of the mean (SEM). The number of repeats (n) indicates the number of patches tested. The open probability of a single channel was calculated as the ratio of the open time and the total recording time (the sum of open and close time). In the case of activity of more than one channel in the patch, the open probability was divided by the number of active channels. Statistical significance was evaluated using a *t*-test (for two groups) or ANOVA with Bonferroni post-hoc test (for more than two groups). Data were compiled using SigmaStat (version 3.5). A value of *P* lower than 0.05 was considered statistically significant.

Results

Nonselective cation channels

The predominant type of ion currents recorded in the cell membrane of mouse fibroblasts were those that passed through nonselective cation channels (Fig. 1A). The activity of these channels was recorded in most (58 %, 15 out of 26) of the patches tested in the inside-out configuration in the symmetrical (in the bath and in the pipette) concentration of 200 mM NaCl. In such conditions, the channels were active in negative and positive voltages carrying the ions in both directions of the membrane. Their unitary conductance (established from the slope of the I/V curve) reached 28 pS. The value of this parameter was lower in the ten-fold gradient of NaCl (200 mM NaCl in the pipette and 20 mM NaCl in the bath) and amounted to 25 pS (Fig. 1B). The conditions used caused decline of the channel activity at positive voltages and an increase in the open probability at negative voltages (Fig. 1D) and indicated that Na^+ ions flowed through the channels in accordance with their electrochemical gradient. The reversal potential obtained from the I/V curve

(Fig. 1C) shifted toward positive values and reached 24 mV – a value closer to the equilibrium potential of sodium ($E_{Na}=54$ mV) than chloride ($E_{Cl}=-44$ mV)

calculated on the basis of ion activities. The above results indicated Na^+ over Cl^- selectivity of the channels.

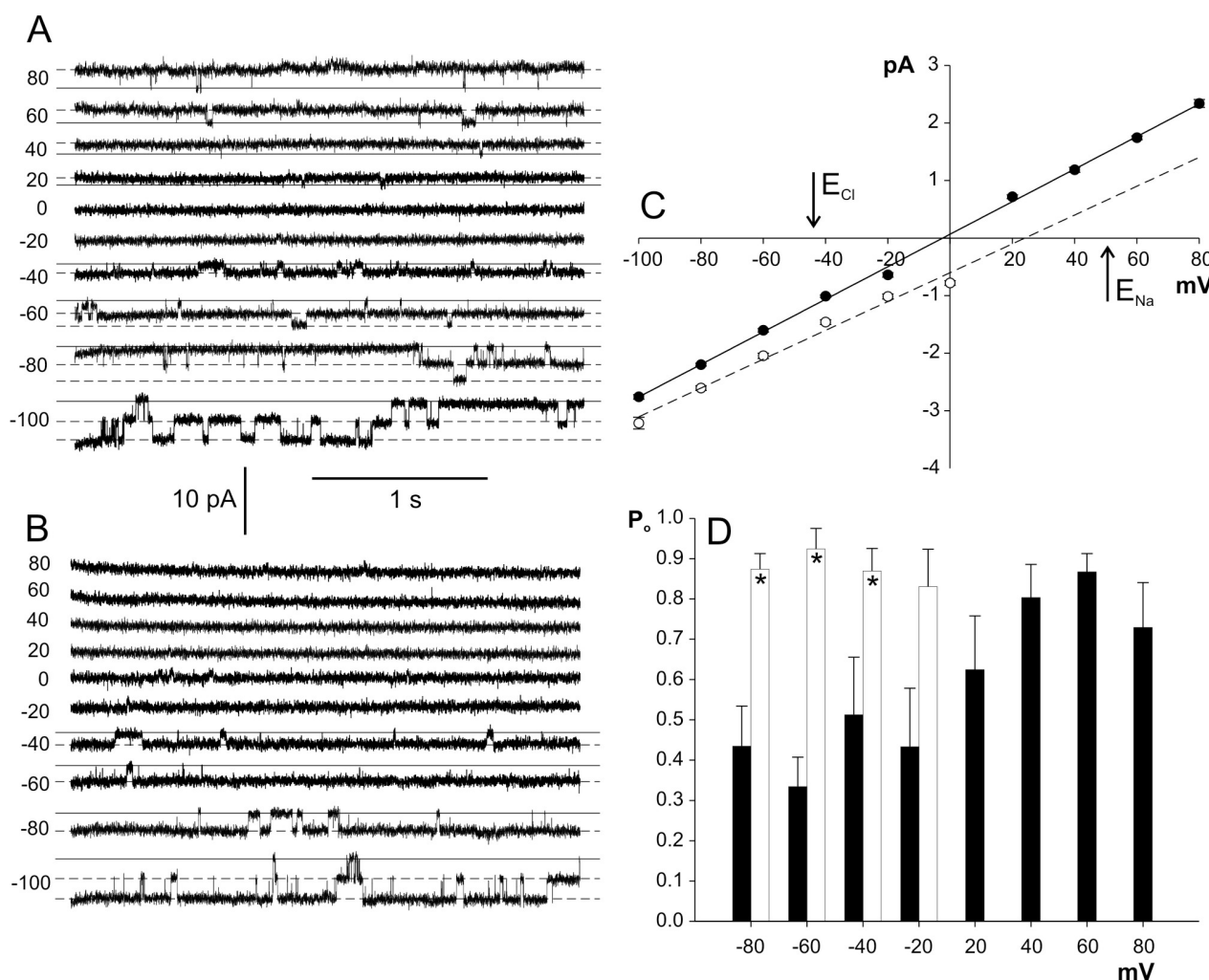


Fig. 1. Activity of nonselective cation channels recorded in the cell membrane from mouse fibroblasts. **(A)** Inside-out recordings carried out in $200 Na^+_{pipette}/200 Na^+_{bath}$. The solid line indicates the closed state of the channels and the dashed line – open states. The values of holding voltages (in mV) are placed on the left side of the traces. **(B)** Recordings obtained after tenfold reduction of the Na^+ concentration in the bath ($200 Na^+_{pipette}/20 Na^+_{bath}$). **(C)** I/V curves obtained in the same conditions as in A (solid line, $n=10$), and B (dashed line, $n=6$). The arrows indicate the reversal potential for Cl^- and Na^+ based on the activity of these ions in the solutions as in B. **(D)** Dependence of the open probability (P_o) of the channels on the voltage applied. The data were obtained in the same conditions as in A (black columns, $n=5$) and B (white columns, $n=5$). The asterisks indicate statistically significant differences ($P < 0.05$). Statistical significance was evaluated using a t -test. The values of P obtained at -80 mV, -60 mV, and -40 mV amounted to 0.003, 0.001, and 0.048, respectively.

The difference between the reversal potential obtained from the measurements and E_{Na} , was the reason for a more detailed study of the low cation-selectivity of the channels. In order to compare the selectivity of the channels to K^+ and Na^+ , a 50-fold gradient facilitating outward K^+ currents and inward Na^+ currents was applied (Fig. 2A). In such conditions, the reversal potential obtained from the I/V curve (Fig. 2C) amounted to -1 mV, which proved that the channels did not distinguish

K^+ and Na^+ ions. In comparison to the experiments carried out in symmetrical concentration $200 Na^+$, the exchange of 200 mM Na^+ on the cytoplasmic side to 200 mM K^+ caused an increase in channel conductance from 28 pS (Fig. 1A, C) to 33 pS (Fig. 2A, C).

Small-conductance K^+ channels

Small-conductance K^+ channel activity was recorded in identical conditions as in the earlier

experiments carried out in the 50-fold gradient of K^+ and Na^+ ($200 Na^+_{pipette}/200 K^+_{bath}$, Fig. 2B, D). These currents were recorded in 36 % (5 of 14) of the patches. The channel conductance was much lower than the conductance of nonselective cation channels and

amounted to 8 pS. The high selectivity of the channels to potassium was confirmed by the value of the reversal potential obtained from the I/V curve (Fig. 2D), which amounted to $-97 mV$ – a value close to the equilibrium potential of potassium ($-100 mV$).

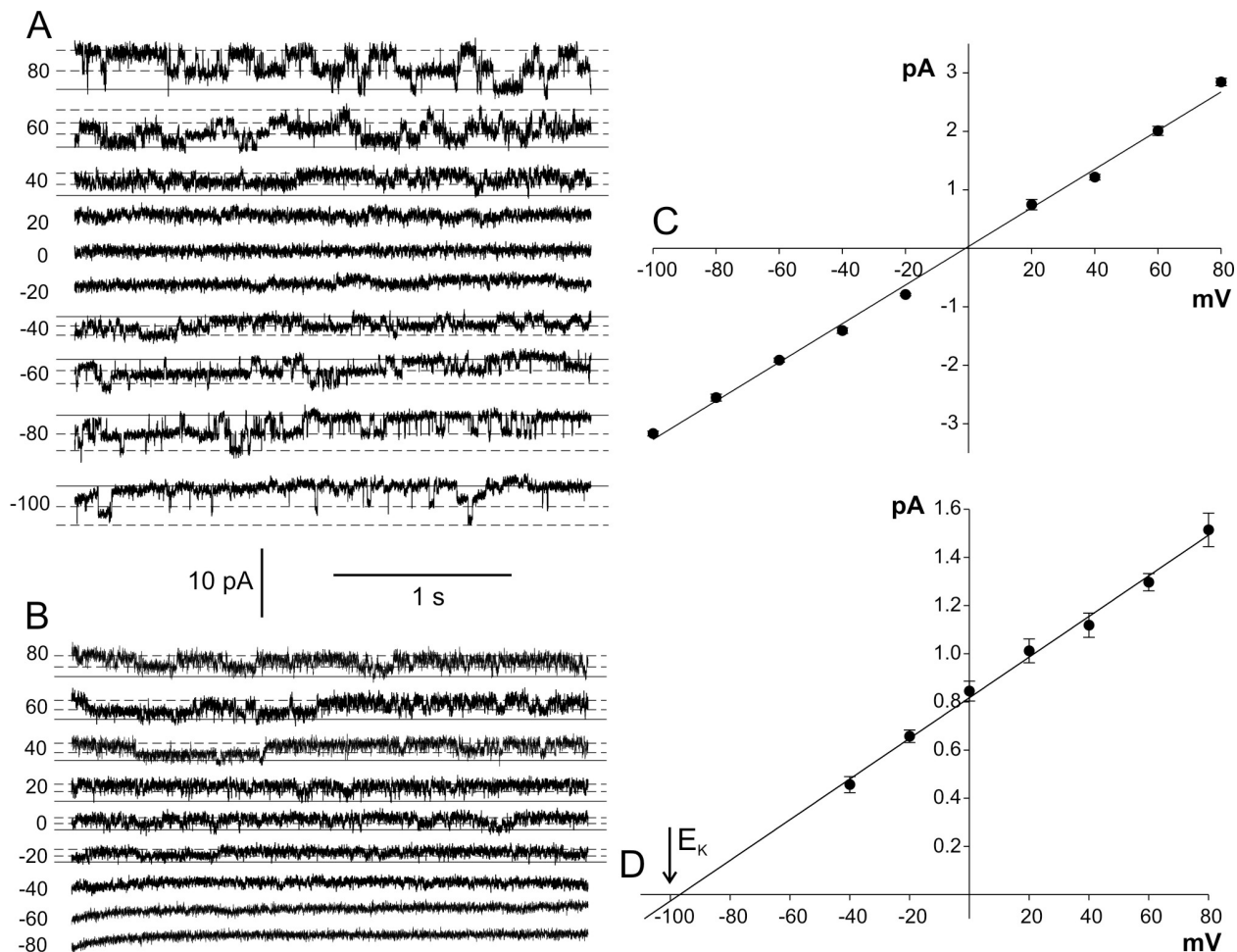


Fig. 2. Permeability of the channels from the cell membrane of mouse fibroblasts to K^+ . **(A)** Inside-out recordings carried out in $200 Na^+_{pipette}/200 K^+_{bath}$. **(B)** Inside-out recordings carried out in the same conditions as in A showing the activity of K^+ selective channels with small conductance. **(C, D)** I/V curves characterizing the cation-permeable channels from A (**C**, $n=5$) and the K^+ selective channels from B (**D**, $n=5$). The arrow indicates the reversal potential for K^+ calculated from the activity of this ion in the solutions.

Large-conductance anion channels

Apart from the channels described previously, large-conductance channels were recorded. These channels recorded in the symmetrical concentration of 200 mM NaCl (Fig. 3A, D) were active in 42 % (11 of 26) of the patches. Interestingly, the channels were not active immediately after excision, but required several minutes of polarization of the patch (by 3-second impulses in the range from $-80 mV$ to $80 mV$ with 20 mV steps). A characteristic trait of the channels was their high conductance amounting to 493 pS. Tenfold reduction of the concentration of cytoplasmic NaCl caused reduction of

the conductance to 296 pS and also a shift of the reversal potential to $-29 mV$, indicating Cl^- over Na^+ selectivity of the channels (Fig. 3B, D). The channels were not highly selective for chloride since their activity was not inhibited by the substitution of cytoplasmic 200 mM Cl^- by 200 mM gluconate – an anion impermeable to chloride channels. The presence of cytoplasmic gluconate instead of Cl^- caused a decrease in conductance from 296 pS to 82 pS, which indicates that the channels are less permeable to gluconate than to chloride (Fig. 3C, D). The relative permeability ratio of gluconate with respect to chloride (P_{glu}/P_{Cl}) was low and reached 0.1.

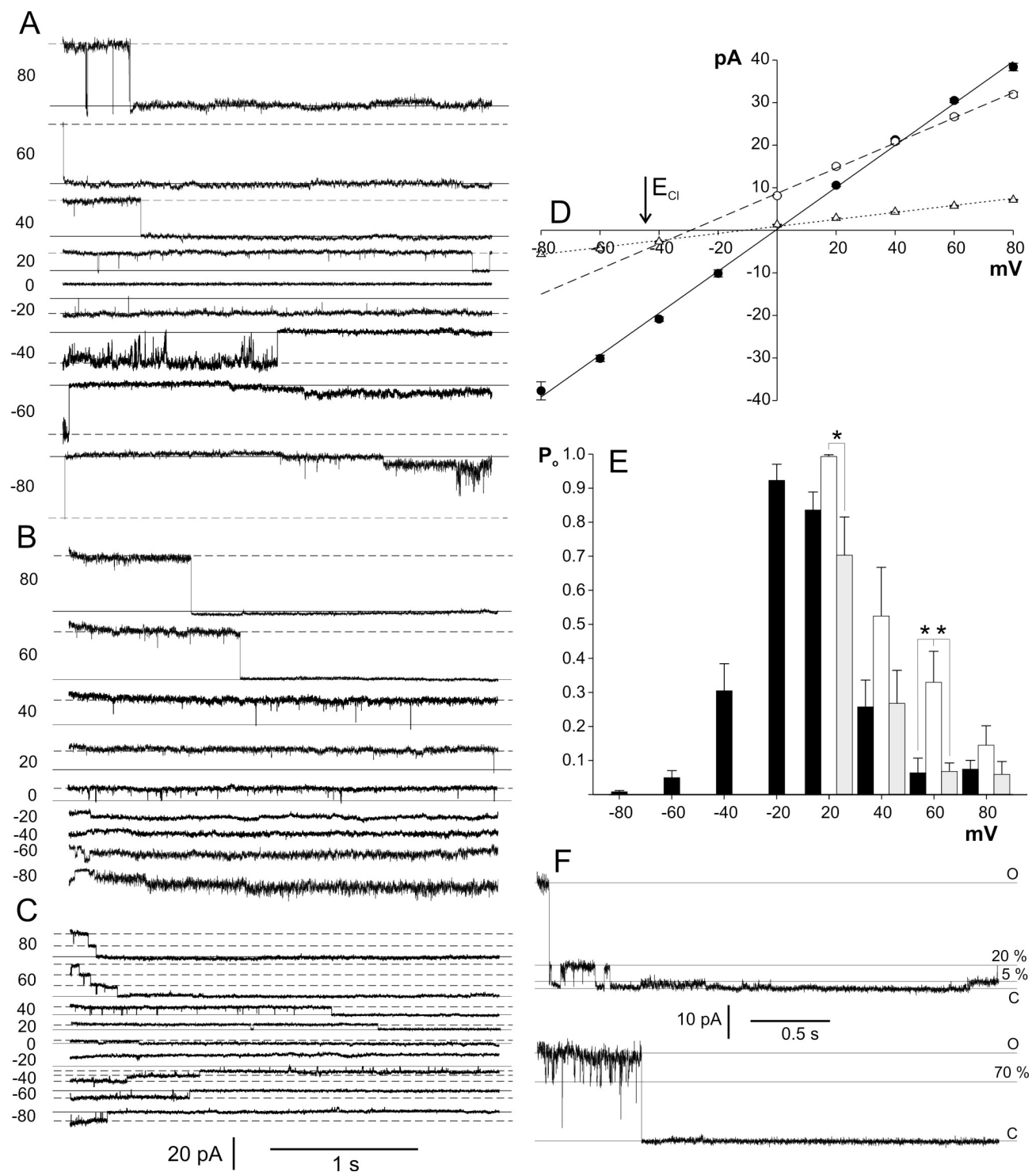


Fig. 3. Activity of large conductance anion channels recorded in the cell membrane from mouse fibroblasts. **(A)** Inside-out recordings carried out in $200 \text{ Na}^+_{\text{pipette}}/200 \text{ Na}^+_{\text{bath}}$. **(B)** Recordings obtained after tenfold reduction of the Na^+ concentration in the bath ($200 \text{ Na}^+_{\text{pipette}}/20 \text{ Na}^+_{\text{bath}}$). **(C)** Recordings showing a decrease in single channel conductance in $200 \text{ Glu}^-_{\text{pipette}}/32 \text{ Cl}^-_{\text{bath}}$. **(D)** I/V curves obtained in the same conditions as in A (solid line, $n=6$), B (dashed line, $n=6$), and C (dotted line, $n=6$). The arrow indicates the reversal potential for Cl^- calculated from the activity of these ions in the solutions as in B. **(E)** Dependence of the open probability (P_o) of the channels on the voltage applied. The data were obtained in the same conditions as in A (black columns, $n=5$), B (white columns, $n=5$), and C (grey columns, $n=5$). The asterisks indicate statistically significant differences ($P < 0.05$). Statistical significance was evaluated using a one-way ANOVA with Bonferroni pairwise multiple comparison. The values of P obtained at 20 mV amounted to 0.043. The values of P obtained at 60 mV amounted to 0.026 (left asterisk) and 0.028 (right asterisk). **(F)** Subconductance levels of large-conductance anion channels. The inside-out recordings obtained at 80 mV (upper panel) and at 60 mV (lower panel) in $200 \text{ Na}^+_{\text{pipette}}/20 \text{ Na}^+_{\text{bath}}$. C and O indicate closed state and open state, respectively. The subconductance levels (5 %, 20 % and 70 %) are indicated.

A characteristic feature of the channels was their activation in the narrow range of voltages, since the open probability of the channels was the highest close to 0 mV (Fig. 3E). The values of this parameter recorded at positive voltages were higher in conditions promoting outward currents carried by Cl^- flowing from the extracellular to the cytoplasmic side of the cell membrane than those obtained in the symmetrical Cl^- concentration. For instance, at 60 mV, the open probability increased from 0.064 ± 0.043 to 0.33 ± 0.091 ($n=5$). The open probability of the channels recorded at positive voltages was also reduced after replacement of extracellular Cl^- with gluconate. The value of this parameter recorded at 60 mV was reduced from 0.33 ± 0.091 to 0.068 ± 0.025 ($n=5$).

During the recordings carried out in a NaCl gradient that reduced cation-permeable channel activity at positive voltages (Fig. 1B, 3B) apart from the main open

level, three subconductance levels of the anion-permeable channels were observed (Fig. 3F). The channel subconductance levels in the presented recordings at positive voltages were 5 % (20 pS), 20 % (75 pS), and 70 % (297 pS).

The range of voltages that activate the channels was studied by application of two kinds of ramp voltages: from -80 mV to +80 mV and from +80 mV to -80 mV. The measurements carried out in the symmetrical Cl^- concentration proved that the channels were activated in a narrow range of voltages (Fig. 4A, B). Even after application of the Cl^- gradient promoting outward currents carried by chloride (Fig. 4C, D), the channels closed at voltages close to 60–70 mV. The ramp protocol used in the measurements of the channel activity after application of the Cl^- gradient allowed estimation of the reversal potential, which was close to E_{Cl} (Fig. 4C, D).

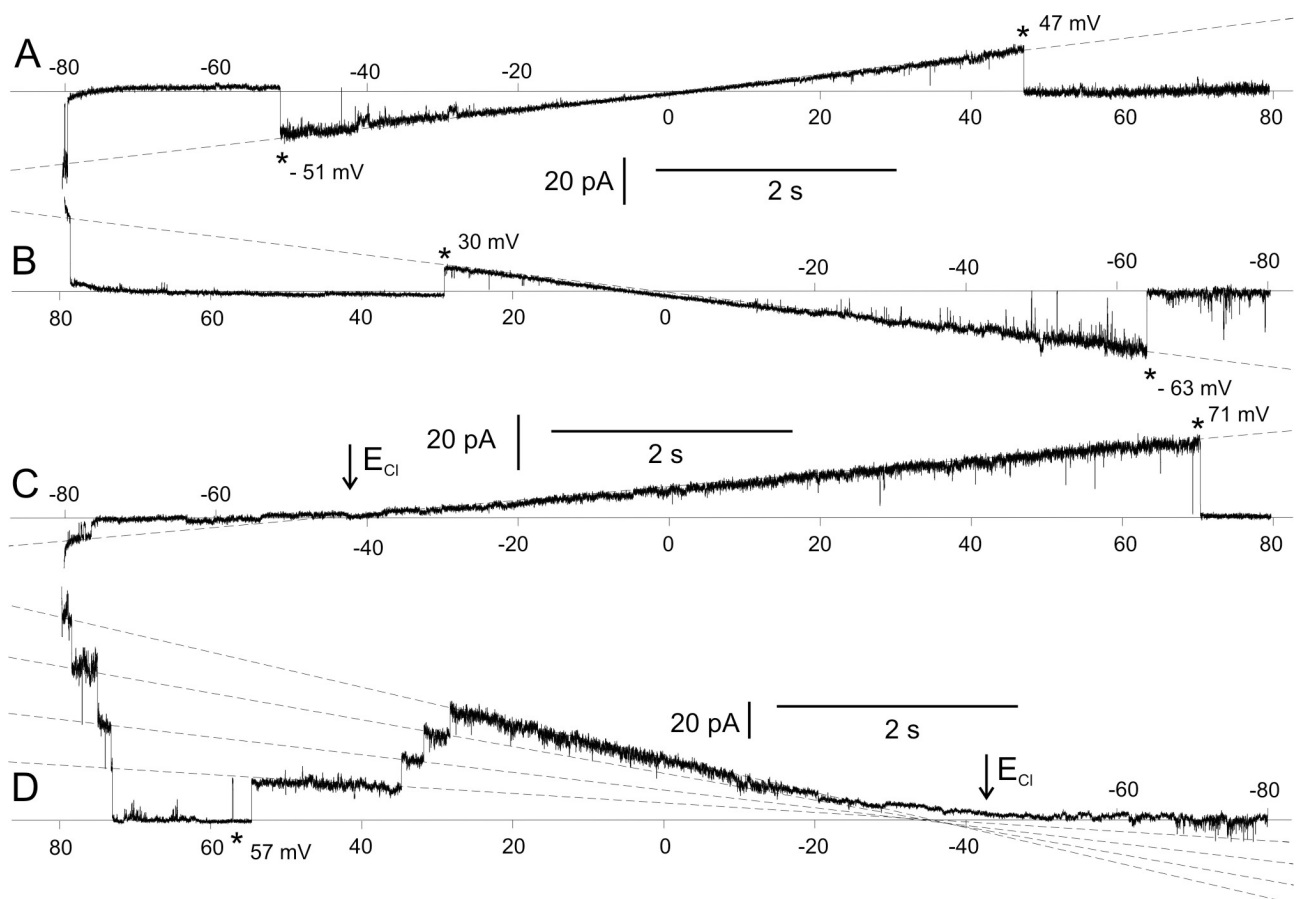


Fig. 4. Activity of large-conductance anion channels recorded during ramp voltages. (A, B) Inside-out recordings obtained in $200 \text{ Na}^+_{\text{pipette}}/200 \text{ Na}^+_{\text{bath}}$. (C, D) Recordings obtained after tenfold reduction of the Na^+ concentration in the bath ($200 \text{ Na}^+_{\text{pipette}}/20 \text{ Na}^+_{\text{bath}}$). The arrows indicate the reversal potential for Cl^- calculated from the activity of this ion in the solutions. The values of the voltage applied (in mV) are placed in the abscissa axis. The dashed lines indicate the open states of the channels and allow determining the reversal potential. The asterisks indicate the value of the voltage that activated the channels.

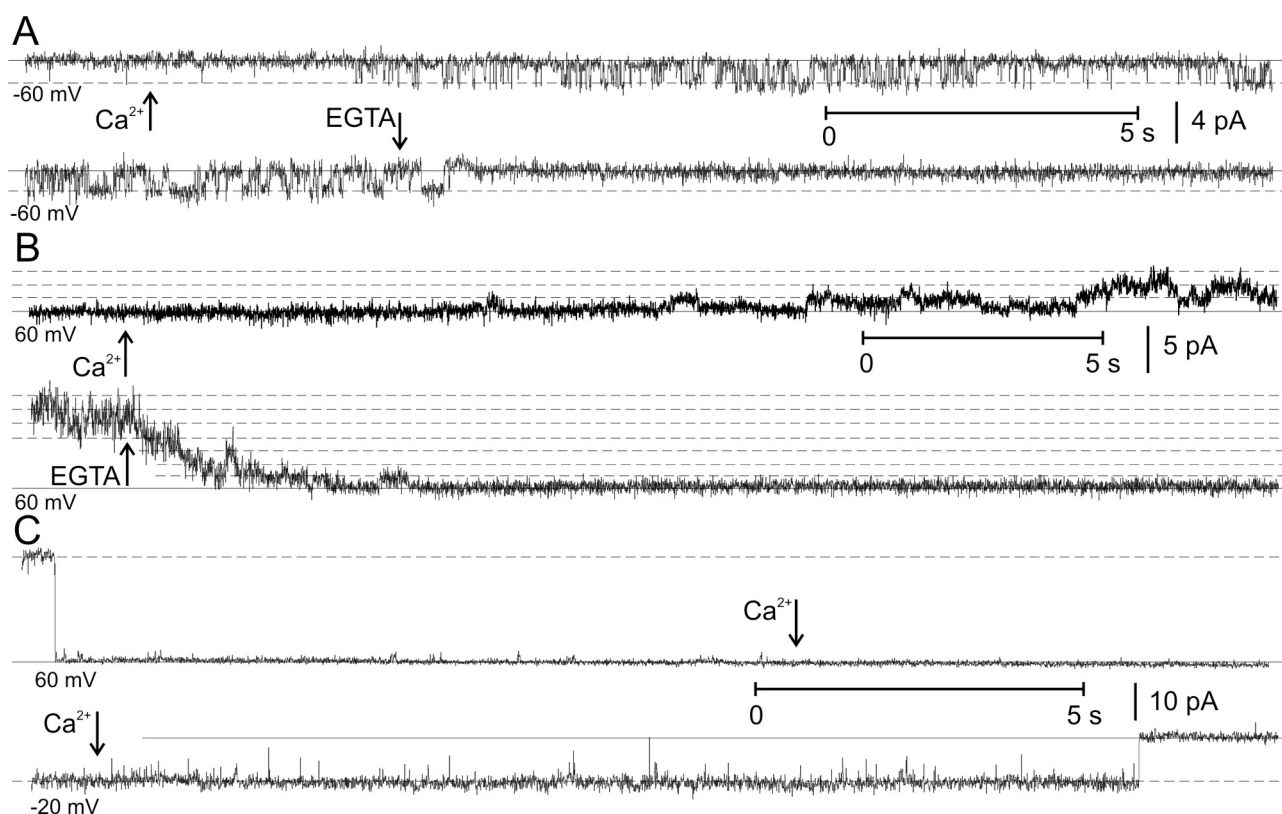


Fig. 5. Calcium dependence of different types of ion currents recorded in mouse fibroblasts. The inside-out measurements were carried out in the absence of Ca^{2+} in the bath (200 Na^+ , $2 \text{ Ca}^{2+}_{\text{pipette}}/200 \text{ K}^+$, $2 \text{ EGTA}_{\text{bath}}$). The calcium dependence was studied for nonselective cation channels (**A**), small-conductance K^+ -selective channels (**B**), and large-conductance anion channels (**C**). The Ca^{2+} -containing solution (200 mM KCl , 4 mM NaCl , 2 mM CaCl_2 , 2 mM MgCl_2 , $\text{pH } 7.3$ buffered with 10 mM HEPES/NaOH) was placed inside a micropipette connected to the pump. During the inside-out recordings, the micropipette was brought close to the patch pipette and the solution was injected. The moment of Ca^{2+} injection is indicated by an arrow. The arrow signed as EGTA indicates the moment of withdrawal of the patch pipette from the stream of the injected Ca^{2+} -containing solution. The values of holding voltages are placed at the bottom of the recordings.

Calcium dependence of the channels

Since internal Ca^{2+} activates some channels found in fibroblasts, e.g. non-selective channels from human skin fibroblasts (Galiotta *et al.* 1989), or potassium channels from rat cardiac fibroblasts (Choi *et al.* 2008), we decided to study the calcium dependence of all channels recorded in the mouse fibroblasts cell line L929. Calcium dependence was studied in a Ca^{2+} -free bath medium by injection of 2 mM Ca^{2+} to the internal site of the membrane during inside-out recordings.

The presence of internal calcium was necessary to maintain the activity of nonselective cation channels. These channels were not recorded in the Ca^{2+} -free bath medium but injection of Ca^{2+} rapidly (within a few seconds) activated the channels (Fig. 5A, upper panel). The channels were also rapidly inactivated after removal of the membrane from the stream of the Ca^{2+} -containing solution (Fig. 5A, lower panel). A relatively long time was necessary for activation of small-conductance K^+ channels (Fig. 5B, upper panel). These channels were

also recorded in a Ca^{2+} -free bath medium within tens of seconds after excision or several or more seconds after chelation of Ca^{2+} by EGTA (Fig. 5B, lower panel). Such results indicate that the Ca^{2+} binding/unbinding process proceeds more slowly in small-conductance potassium channels than in nonselective cation channels. No calcium dependence was observed in the large-conductance anion channels (Fig. 5C). Injection of Ca^{2+} neither opened the channels at voltages which usually caused their inactivation (Fig. 5C, upper panel) nor changed the channels' activity recorded at voltages close to zero (Fig. 5C, lower panel). The results indicate that voltage but not calcium is the main factor that regulates the activity of large-conductance anion channels.

Discussion

In this study carried out on the membrane of the mouse fibroblast cell line L929, three different ion channel activities were observed. Most often, the activity

of nonselective cation channels was recorded. The channel selectivity did not allow distinguishing between sodium and potassium. Similar channels nonselective for cations activated by a platelet-derived growth factor were previously described in mouse fibroblasts in the LMTK⁻ cell line (Frace and Gargus 1989). Apart from the equal selectivity for basic monovalent cations, a common feature of the channels from the LMTK⁻ and L929 cell lines was their conductance amounting to 28 pS for both channels. Another parameter that can be taken into account in the comparison of both channels is their voltage dependence. Channels from the L929 cell line recorded in symmetrical concentration 200 mM NaCl opened with a high open probability at positive voltages (Fig. 1D), while the channels from the LMTK⁻ cell line were voltage independent. On the other hand, the voltage dependence of the channels determined in this study is similar to sodium and potassium nonselective channels from human fibroblasts, which opened with a higher probability at positive voltages and passed the cations with the conductance of 14 to 25 pS (Galiotta *et al.* 1989). Moreover, in contrast to the channels from the LMTK⁻ cell line, the channels from the human fibroblasts and L929 cell line were activated by cytoplasmic calcium. It seems that the voltage and calcium dependence of nonselective cation channels is not a common feature of channels from different organisms or even from different cell lines.

The second type of the channels recorded in our study was the small-conductance K⁺ channel characterised by low conductance reaching 8 pS (Fig. 2) and Ca²⁺ dependence (Fig. 6B). According to the present knowledge, there are no similar channels in mammalian fibroblasts and it is hard to classify the channels to other known types of channels. The main features of the small-conductance K⁺ channels analysed in this study are similar to small conductance Ca²⁺-activated K⁺ channels (SK channels) encoded by at least three genes: *SK1*, *SK2*, and *SK3* (Kohler *et al.* 1996). Apart from small unitary conductance (2-20 pS), Ca²⁺ sensitivity (submicromolar concentrations), weak voltage dependence, and susceptibility to blockade by d-tubocurarine and apamin are characteristic for SK channels (Kohler *et al.* 1996, Xia *et al.* 1998, Hirschberg *et al.* 1999, Soh and Park 2002). All the three subtypes of SK are present in mouse atrial and ventricular myocytes (Tuleja *et al.* 2005), where heteromeric SK2-SK3 channels contribute to action potential repolarization (Hancock *et al.* 2015). In turn, in mouse urinary bladder, the *SK2* gene is expressed

and is essential for regulation of the smooth muscle contractility by SK channels (Thorneloe *et al.* 2008).

The third type of the channels recorded in our study was the large-conductance anion channel (Fig. 3). Similar channels were recorded and characterized earlier in different cell types, including human fibroblasts (Nobile and Galiotta 1988). Apart from the large conductance of the channels from mouse (493 pS in the symmetrical concentration of 200 mM NaCl) and human (300 pS in symmetrical 135 mM NaCl), a common feature of the channels was their similar voltage dependence, since the channels from human fibroblasts were usually open at voltages between -20 to +20 mV and more positive or negative voltages closed the channels. A bell-shaped curve of the open probability with the highest value of this parameter at the voltage close to the reversal potential/zero mV was found in large-conductance anion channels from other types of cultured cells, for instance in human T-lymphocytes (Pahapill and Schlichter 1992), rabbit colonic smooth muscle (Sun *et al.* 1992), or pigmented ciliary epithelial (PCE) cells (Mitchell *et al.* 1997). Moreover, the activity of a large-conductance channel from PCE was also recorded several minutes after polarization, similar to the one recorded in this study. The next feature of large-conductance channels, similar to the channels recorded in this study, is their low selectivity and nearly equal permeability to gluconate and other anions like I, Br, NO₃, F, SCN, glucuronate, HCO₃, aspartate and acetate (Stumpff *et al.* 2009, Bosma 1989, Dixon *et al.* 1993). The relative permeability ratio of gluconate in respect to Cl⁻ obtained by Stumpff and coworkers from ruminal epithelial cells from sheep ($P_{glu}/P_{Cl}=0.16$; Stumpff *et al.* 2009), was close to the value of this parameter obtained in our study ($P_{glu}/P_{Cl}=0.1$). Besides gluconate, low permeability ratios of aspartate and fluoride in respect to chloride were recorded in channels from a mouse B lymphocyte cell line ($P_{aspartate}/P_{Cl}=0.62$; Bosma 1989), and muscle vesicles prepared from *Ascaris suum* ($P_F/P_{Cl}=0.52$; Dixon *et al.* 1993). Large-conductance channels from a mouse B lymphocyte and the channels characterized in this study possess another similar feature – the existence of three subconductance levels. Among the three subconductance levels recorded in mouse B lymphocyte reaching 30 %, 55 %, and 75 % of the total conductance, one was close to that recorded in our study (70 %, Fig. 3F). Subconductance levels were also recorded in the channels from other kinds of cells like the Golgi complex from rat liver (Thompson *et al.* 2002),

human L-lymphocytes (Pahapill and Schlichter 1992), rat cardiac myocytes (Coulombe and Coraboeuf 1992), rat cortical astrocytes (Jalonen 1993), and rabbit colonic smooth muscle (Sun *et al.* 1992).

In conclusion, this study has proved the existence of three different ion channel types in mouse fibroblasts, which exhibit common features with known channels of other cells/cell lines. Three channel types with known physiological functions are the candidates for being active in mouse fibroblasts: non-selective for cations, small-conductance Ca²⁺-activated K⁺ channels

(SK), and a large-conductance anion channels. This work is a basis for a more detailed study of the channels from mouse L929 line cells.

Conflict of Interest

There is no conflict of interest.

Acknowledgements

This study was funded by the Scientific Research Fund of Maria Curie-Skłodowska University and the Medical University of Lublin.

References

- BOSMA MM: Anion channels with multiple conductance levels in a mouse lymphocyte-B cell-line. *J Physiol* **410**: 67-90, 1989.
- CHOI S, LEE W, YUN J, SEO J, LIM I: Expression of Ca²⁺-activated K⁺ channels and their role in proliferation of rat cardiac fibroblasts. *Korean J Physiol Pharmacol* **12**: 51-58, 2008.
- COULOMBE A, CORABOEUF E: Large-conductance chloride channels of newborn rat cardiac myocytes are activated by hypotonic media. *Pflug Arch Eur J Phy* **422**: 143-150, 1992.
- DIXON DM, VALKANOV M, MARTIN RJ: A patch-clamp study of the ionic selectivity of the large conductance, Ca-activated chloride channel in muscle vesicles prepared from *Ascaris suum*. *J Membrane Biol* **131**: 143-149, 1993.
- DOROSHENKO P: High intracellular chloride delays the activation of the volume-sensitive chloride conductance in mouse L-fibroblasts. *J Physiol* **514**: 437-446, 1999.
- ESTACION M: Characterization of ion channels seen in subconfluent human dermal fibroblasts. *J Physiol* **436**: 579-601, 1991.
- ETCHEBERRIGARAY R, ITO E, OKA K, TOFELGREHL B, GIBSON GE, ALKON DL: Potassium channel dysfunction in fibroblasts identifies patients with Alzheimer disease. *Proc Natl Acad Sci U S A* **90**: 8209-8213, 1993.
- FISKE JL, FOMIN VP, BROWN ML, DUNCAN RL, SIKES RA: Voltage-sensitive ion channels and cancer. *Cancer Metast Rev* **25**: 493-500, 2006.
- FRACE AM, GARGUS JJ: Activation of single-channel currents in mouse fibroblasts by platelet-derived growth factor. *Proc Natl Acad Sci U S A* **86**: 2511-2515, 1989.
- GALIETTA LJV, MASTROCOLA T, NOBILE M: A class of non-selective cation channels in human fibroblasts. *FEBS Lett* **253**: 43-46, 1989.
- GOODWIN PA, CAMPBELL KE, EVANS BAJ, WANN KT: In vitro patch-clamp studies in skin fibroblasts. *J Pharmacol Toxicol* **39**: 229-233, 1998.
- HANCOCK JM, WEATHERALL KL, CHOISY SC, JAMES AF, HANCOX JC, MARRION NV: Selective activation of heteromeric SK channels contributes to action potential repolarization in mouse atrial myocytes. *Heart Rhythm* **12**: 1003-1015, 2015.
- HIRSCHBERG B, MAYLIE J, ADELMAN JP, MARRION NV: Gating properties of single SK channels in hippocampal CA1 pyramidal neurons. *Biophys J* **77**: 1905-1913, 1999.
- HOSOI S, SLAYMAN CL: Membrane voltage, resistance, and channel switching in isolated mouse fibroblasts (L-cells) - a patch-electrode analysis. *J Physiol* **367**: 267-290, 1985.
- JALONEN T: Single-channel characteristics of the large-conductance anion channel in rat cortical astrocytes in primary culture. *Glia* **9**: 227-237, 1993.
- KOHLER M, HIRSCHBERG B, BOND CT, KINZIE JM, MARRION NV, MAYLIE J, ADELMAN JP: Small-conductance, calcium-activated potassium channels from mammalian brain. *Science* **273**: 1709-1714, 1996.

- MITCHELL CH, WANG L, JACOB TJC: A large-conductance chloride channel in pigmented ciliary epithelial cells activated by GTP γ S. *J Membrane Biol* **158**: 167-175, 1997.
- NOBILE M, GALIETTA LJV: A large conductance Cl $^-$ channel revealed by patch-recordings in human fibroblasts. *Biochem Biophys Res Commun* **154**: 719-726, 1988.
- PAHAPILL PA, SCHLICHTER LC: Cl $^-$ channels in intact human T lymphocytes. *J Membrane Biol* **125**: 171-183, 1992.
- PERES A, STURANI E, ZIPPEL R: Properties of the voltage-dependent calcium-channel of mouse Swiss 3T3 fibroblasts. *J Physiol* **401**: 639-655, 1988a.
- PERES A, ZIPPEL R, STURANI E, MOSTACCIUOLO G: A voltage-dependent calcium current in mouse Swiss 3T3 fibroblasts. *Pflug Arch Eur J Phy* **411**: 554-557, 1988b.
- PEREZ-REYES E: Molecular physiology of low-voltage-activated T-type calcium channels. *Physiol Rev* **83**: 117-161, 2003.
- REPP H, KOSCHINSKI A, DECKER K, DREYER F: Activation of a Ca $^{2+}$ -dependent K $^+$ current in mouse fibroblasts by lysophosphatidic acid requires a pertussis toxin-sensitive G protein and Ras. *Naunyn Schmiedebergs Arch Pharmacol* **358**: 509-517, 1998.
- SOH H, PARK CS: Localization of divalent cation-binding site in the pore of a small conductance Ca $^{2+}$ -activated K $^+$ channel and its role in determining current-voltage relationship. *Biophys J* **83**: 2528-2538, 2002.
- STUMPF F, MARTENS H, BILK S, ASCHENBACH JR, GAEBEL G: Cultured ruminal epithelial cells express a large-conductance channel permeable to chloride, bicarbonate, and acetate. *Pflug Arch Eur J Phy* **457**: 1003-1022, 2009.
- SUN XP, SUPPLISSON S, TORRES R, SACHS G, MAYER E: Characterization of large-conductance chloride channels in rabbit colonic smooth-muscle. *J Physiol* **448**: 355-382, 1992.
- THEERAKITTAYAKORN K, BUNPRASERT T: Differentiation capacity of mouse L929 fibroblastic cell line compare with human dermal fibroblast. *World Acad Sci Eng Technol* **50**: 373-376, 2011.
- THOMPSON RJ, NORDEEN MH, HOWELL KE, CALDWELL JH: A large-conductance anion channel of the Golgi complex. *Biophys J* **83**: 278-289, 2002.
- THORNELOE KS, KNORN AM, DOETSCH PE, LASHINGER ESR, LIU AX, BOND CT, ADELMAN JP, NELSON MT: Small-conductance, Ca $^{2+}$ -activated K $^+$ channel 2 is the key functional component of SK channels in mouse urinary bladder. *Am J Physiol Regul Integr Comp Physiol* **294**: R1737-R1743, 2008.
- THOROED SM, BRYAN-SISNEROS A, DOROSHENKO P: Protein phosphotyrosine phosphatase inhibitors suppress regulatory volume decrease and the volume-sensitive Cl $^-$ conductance in mouse fibroblasts. *Pflug Arch Eur J Phy* **438**: 133-140, 1999.
- TUTEJA D, XU DY, TIMOFEYEV V, LU L, SHARMA D, ZHANG Z, XU YF, NIE LP, VAZQUEZ AE, YOUNG JN, GLATTER KA, CHIAMVIMONVAT N: Differential expression of small-conductance Ca $^{2+}$ -activated K $^+$ channels SK1, SK2, and SK3 in mouse atrial and ventricular myocytes. *Am J Physiol Heart Circ Physiol* **289**: H2714-H2723, 2005.
- XIA XM, FAKLER B, RIVARD A, WAYMAN G, JOHNSON-PAIS T, KEEN JE, ISHII T, HIRSCHBERG B, BOND CT, LUTSENKO S, MAYLIE J, ADELMAN JP: Mechanism of calcium gating in small-conductance calcium-activated potassium channels. *Nature* **395**: 503-507, 1998.
-